Synthesis of Axially Chiral Bibenzo[*g*]coumarin Derivatives by Rhodium-Catalyzed Oxidative Annulation of Thiocarbamates

Ryo Takishima [a]
Koushik Ghosh [a]
Yuji Nishii *[a,b]
Masahiro Miura *[c]

[a] Department of Applied Chemistry, Graduate School of Engineering, Osaka University, Suita, Osaka 565-0871, Japan

[b] Center for Future Innovation, Graduate School of Engineering, Osaka University, Suita, Osaka 565-0871, Japan.

[c] Innovative Catalysis Science Division, Institute for Open and Transitionary Research Initiatives (ICS-OTRI), Osaka University, Suita, Osaka 565-0871, Japan.

y_nishii@chem.eng.osaka-u.ac.jp
miura@chem.eng.osaka-u.ac.jp

Click here to insert a dedication.

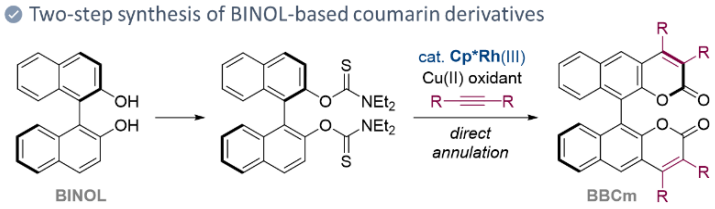

Received:
Accepted:
Published online:
DOI:

Abstract Polyaromatic organic compounds have attracted significant attention because of their wide application in various functional materials. Recently, transition-metal-catalyzed C–H activation and the subsequent oxidative cyclization with unsaturated compounds has emerged as a promising synthetic method for multi-ring systems. We herein report two-step synthesis of binaphthyl-fused chiral bibenzo[*g*]coumarin derivatives by Rh-catalyzed annulative coupling reaction of BINOL-based thiocarbamate with alkynes. Optical properties of the coupling products were evaluated.

Key words coumarin, rhodium; C–H activation; BINOL; circular dichroism

Poly(hetero)aromatic compounds have attracted considerable research interest because of their substantial importance for functional organic materials such as light-emitting materials, semiconductors, solar cells, etc. To meet the increasing demand, development of new efficient synthetic methods has been a hot topic in organic chemistry field. The last few decades witnessed a significant progress in transition-metal-catalyzed C–H activation chemistry, and the subsequent oxidative cyclization of metallacycle species with unsaturated compounds has been extensively studied.[1] In 2007, Satoh and Miura first utilized a Cp*Rh(III) complex $[Cp^*RhCl_2]_2$ as the catalyst for direct oxidative annulation of benzoic acid derivatives with internal alkynes to produce the corresponding isocoumarins (Scheme 1a).[2] Afterward, Jones reported isoquinoline salt synthesis with stoichiometric Cp*Rh(III) complex,[3] and Fagnou developed catalytic reaction systems for synthesizing indoles and isoquinolines (Scheme 1b and 1c).[4] These initial reports and many excellent works by other leading practitioners have positioned the Cp*Rh(III) as well as relevant Co and Ir catalysts as one of the most promising synthetic tools for the direct C–H functionalization.

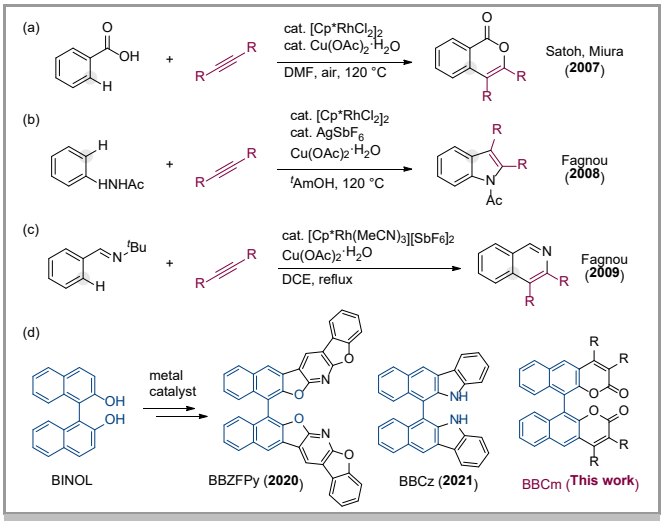

Scheme 1 Catalytic Synthesis of Benzo-Fused Heterocycles

Recently, pure organic functional materials bearing chiroptical characteristics have attracted widespread attention.[5] BINOL (1,1'-bi-2-naphthol) has been commonly utilized as the chiral scaffold because of its availability and the possibility of site-selective functionalization. Our group previously achieved the synthesis of BINOL-based bibenzofuro[2,3-*b*:3′,2′-*e*]pyridine (BBZFPy), and bibenzo[*b*]carbazole (BBCz) derivatives adopting metal-catalyzed direct C–H functionalization as the key reaction (Scheme 1c).[6] Meanwhile, coumarin (1-benzopyran-2-one) derivatives have been among the most important O-heterocyclic compounds which have been applied in chemosensors, light-emitting devices, and laser dyes.[7] In this manuscript, we report the synthesis of new binaphthyl-fused chiral bibenzo[*g*]coumarin (BBCm) derivatives.[8] The coumarin ring formation was achieved by the Rh-catalyzed oxidative annulation of aryl thiocarbamate with alkynes, which was independently developed by Xia and Satoh/Miura groups.[9,10] Both enantiomers were obtained as

optically pure forms from commercially available BINOL in two steps, and their optical properties were evaluated.

The target axially chiral coumarin derivatives were synthesized from the commercially available (*R*)-BINOL in two steps: directing group installation and the Rh-catalyzed oxidative annulation with alkynes (Scheme 2). The hydroxyl groups of (*R*)-BINOL were protected as thiocarbamate upon treatment with NaH and diethylthiocarbamoyl chloride to give (*R*)-**1** in 45% yield. A relatively long reaction time was required because the BINOL functionalization should be conducted below 80 °C in order to avoid racemization of binaphthyl scaffold.[11] This compound was subsequently coupled with diphenylacetylene **2a** in the presence of $[Cp^*RhCl_2]_2$ catalyst, $AgSbF_6$ additive, and Cu oxidant in heating dioxane/diglyme solvent (see the Supporting Information for optimization study). To our delight, the target coupling product (*R*)-**3a** was obtained in 55% yield as optically pure form. Several diarylacetylenes were also applicable to the reaction and gave the corresponding BBCm derivatives (*R*)-**3a**–**3f** in moderate to good yields (25~70%). Alkynes bearing electron donating group (**2b**, **2c**) were relatively productive than electron deficient ones (**2d**, **2e**). We also synthesized the corresponding *S*-isomers similarly to the *R*-isomers.

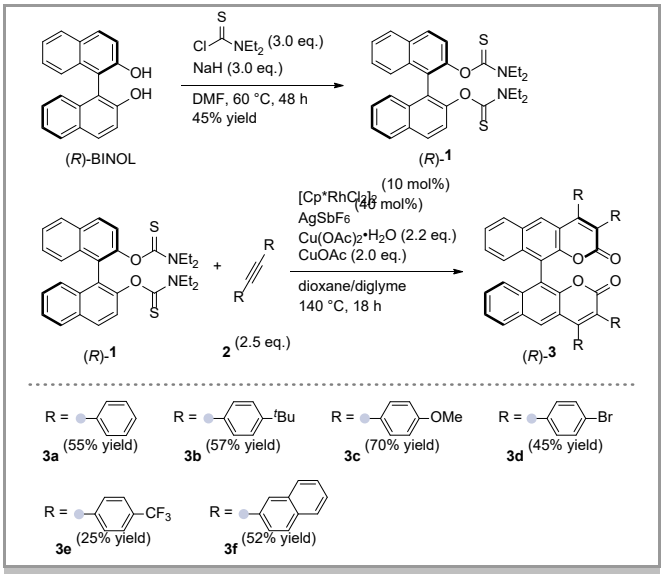

Scheme 2 Synthesis of Bibenzo[*g*]coumarin Derivatives 3.

We then evaluated optical properties of the obtained coumarin derivatives, and the results were summarized in Figure 1 and Table 1. The benchmark compound **3a** exhibited blue-green fluorescence at around 450 nm with a quantum efficiency Φ = 0.13 as the $CHCl_3$ solution. In the solid state, the absorption band was considerably red-shifted whereas the emission spectral shape did not change significantly as compared to those of the $CHCl_3$ solution. These results suggested that **3a** undergoes significant conformational change upon excitation in solution state. In fact, the binaphthyl dihedral angle within **3a** calculated by DFT is 79.4 ° in the ground state, whereas 60.9 ° in the excited state S1. The simulated fluorescence spectrum agrees well with the measured spectrum of **3a**, indicating that the emission is of unimolecular rather than of an aggregated state (see the Supporting Information). We assume that the conformation of **3a** in the solid state would be similar to that of the excited state, thereby exhibiting similar fluorescence character. Unfortunately, **3a** as well as **3b**–**3f** were amorphous compounds, and thus their packing structures have not been obtained by the X-ray crystallographic analysis. A similar trend was observed in the absorption/fluorescence spectra of **3b**–**3f** whereas their quantum efficiencies were somewhat lower than **3a**.

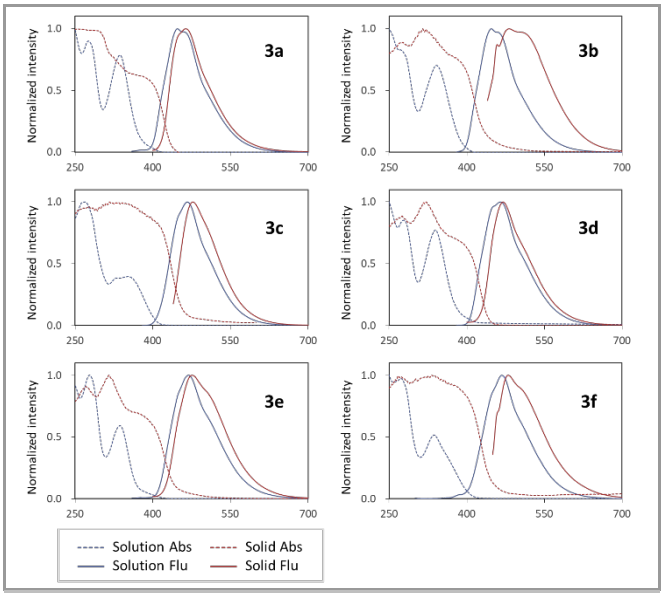

Figure 1 Absorption (dotted lines) and fluorescence (solid lines) spectra of **3** measured as $CHCl_3$ solutions (1.0×10^{-5} M, blue) and in solid states (red).

Table 1 Summary of Optical Properties.

	solution			solid state		
	$\lambda_{max/abs}$	$\lambda_{max/flu}$	Φ_{flu}	$\lambda_{max/abs}$	$\lambda_{max/flu}$	Φ_{flu}
3a	337 nm	448 nm	0.13	300 nm	464 nm	0.10
3b	341 nm	446 nm	0.04	316 nm	483 nm	0.06
3c	354 nm	467 nm	0.08	337 nm	478 nm	0.21
3d	339 nm	465 nm	0.03	321 nm	470 nm	0.01
3e	338 nm	469 nm	0.04	315 nm	476 nm	0.03
3f	336 nm	468 nm	0.05	332 nm	480 nm	0.04

[a] Measured as $CHCl_3$ solutions (1.0×10^{-5} M).

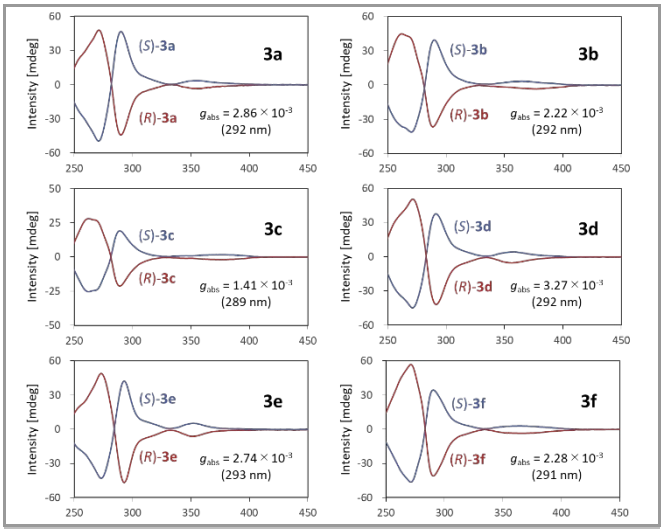

Figure 2 CD spectra measured as $CHCl_3$ solutions (1.0×10^{-5} M).

Next, chiroptical properties of the coupling products were examined. The circular dichroism (CD) spectra of **3a**–**3f** as diluted $CHCl_3$ solutions (1.0×10^{-5} M) are reported in Figure 2.

All compounds showed similar spectral shape, and each pair of (*S*)- and (*R*)-enantiomers apparently draws mirror image, affording relatively large anisotropy factors g_{abs} on the order of 10^{-3}. Characteristic Cotton signals at the wavelength range from 250 to 300 nm were typical of axially chiral binaphthyl compounds.[12]

We also measured the circularly polarized luminescence (CPL) spectra of compounds **3**; however, obvious mirror images were not obtained both in solution and solid states (see the Supporting Information). The spectrum of **3c** as $CHCl_3$ solution was relatively discernible but a promising anisotropy factor value g_{lum} was not determined.

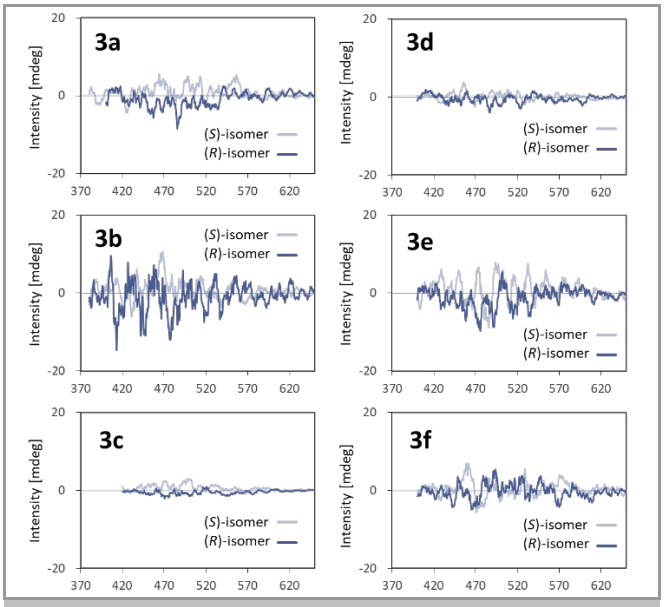

Figure 3 CPL spectra measured as $CHCl_3$ solutions (1.0×10^{-5} M).

In summary, we synthesized new binaphthyl-fused chiral BBCm derivatives by Rh-catalyzed annulative coupling of thiocarbamate with alkynes. Both enantiomers were obtained as optically pure forms from commercially available BINOL in two steps. The products **3** gave clear mirror images in CD spectra, whereas their CPL activity was insufficient. Further study on the synthesis and chiroptical characteristics of binaphthyl-fused polyaromatic compounds is currently underway in our group.

Funding Information

This research was supported by a Grant-in-Aid for Scientific Research from JSPS (Specially Promoted Research, Grant No. JP 17H06092).

Supporting Information

YES (this text will be updated with links prior to publication)

Primary Data

NO.

Conflict of Interest

The authors declare no conflict of interest.

References and Notes

Experimental procedures and characterization data

Preparation of 1: To a 50 mL two-necked round-bottom flask equipped with an N_2 balloon were added (*S*)- or (*R*)-BINOL (804 mg, 3.0 mmol), NaH (540 mg, 9.0 mmol), diethylthiocarbamoyl chloride (1.37 g, 9.0 mmol), and DMF (12.0 mL). The mixture was stirred at 60 °C for 48 h with an oil bath. The resulting mixture was poured into water and extracted with EtOAc three times. The combined organic layer was washed with brine, dried over Na_2SO_4, and concentrated in vacuo. The residue was purified by silica gel column chromatography (hexane/EtOAc = 4/1) and GPC ($CHCl_3$) to give the title compound as white solid; (*R*)-**1** (700 mg, 45% yield), (*S*)-**1** (622 mg, 40% yield).

Melting point: 106-108 °C; ^{1}H NMR (400 MHz, $CDCl_3$) δ 7.94 (d, *J* = 8.84 Hz, 2H), 7.87 (d, *J* = 8.16 Hz, 2H), 7.57 (d, *J* = 8.92 Hz, 2H), 7.51 (d, *J* = 8.44 Hz, 2H), 7.43 (td, *J*= 7.5, 1.16, 2H), 7.29 (td, *J*= 7.5, 1.18, 2H), 3.65-3.40 (m, 4H), 3.11-2.80 (m, 4H), 0.89 (t, *J* = 7.08 Hz, 6H), 0.57 (t, *J* = 7.08 Hz, 6H); ^{13}C NMR (100 MHz, $CDCl_3$) δ 185.15, 149.48, 133.36, 131.50, 128.21, 127.62, 126.97, 126.32, 125.68, 124.09, 123.73, 47.44, 43.40, 12.65, 11.26; HRMS (APCI) *m/z*: $[M+H]^+$ Calcd for $C_{30}H_{33}N_2O_2S_2$ 517.1977; Found 517.1948; CHIRAL ART Amylose-SA column, *n*-hexane/chloroform = 90/10, 0.5 mL/min, 25 °C, (*R*)-**1**: t_R = 29.66 min, (*S*)-**1**: t_R = 43.35 min, UV detection at 250.0 nm.

General Procedure for the Rh-catalyzed Oxidative Annulation: To an oven-dried 10 mL screw-top tube were added (*R*)-**1** (51.7 mg, 0.1 mmol), alkyne **2** (0.25 mmol), $[CpRhCl_2]_2$ (6.2 mg, 0.01 mmol), $AgSbF_6$ (13.7 mg, 0.04 mmol), $Cu(OAc)_2$ (40 mg, 0.22 mmol), and $Cu(OAc)_2{\cdot}H_2O$ (40 mg, 0.20 mmol). The tube was filled with N_2. Diglyme (2.0 mL) and 1,4-dioxane (2.0 mL) were added via syringe, and the mixture was heated at 140 °C with an oil bath for 18 h. The resulting mixture was filtered through a pad of Celite eluting with EtOAc. The filtrate was concentrated in vacuo, and the residue was purified by silica gel column chromatography (hexane/EtOAc = 4/1) and GPC ($CHCl_3$) to give (*R*)-**3**. The corresponding *S*-isomers were synthesized similarly in small batches for analyses.

(*R*)-3,3',4,4'-tetraphenyl-2*H*,2'*H*-[10,10'-bibenzo[*g*]chromene]-2,2'-dione ((*R*)-**3a**)

White solid (38 mg, 55% yield), melting point > 300 °C; ^{1}H NMR (400 MHz, $CDCl_3$) δ 7.14-7.20 (m, 10H), 7.22-7.24 (m, 2H), 7.28-7.30 (m, 2H), 7.35-7.46 (m, 12H), 7.87 (d, *J* = 8.2 Hz, 2H), 7.92 (s, 2H); ^{13}C NMR (100 MHz, $CDCl_3$) δ117.2, 121.0, 125.46, 125.58, 127.65, 127.72, 128.31, 128.47, 128.61, 129.31, 129.53, 129.62, 129.79, 130.59, 134.14, 134.26, 134.77, 148.15, 151.56, 161.01; HRMS (APCI) *m/z*: $[M+H]^+$ Calcd for $C_{50}H_{31}O_4$ 695.2217; Found 695.2211; $[\alpha]^{20}_D$ = +92.9 (*S*-isomer), -94.4 (*R*-isomer) as $CHCl_3$ solution (*c* = 0.1). CHIRAL ART Amylose-SA column, *n*-hexane/chloroform = 70/30, 0.2 mL/min, 25 °C, (*S*)-**3a**: t_R = 27.17 min, (*R*)-**3a**: t_R = 23.14 min, UV detection at 250.0 nm.

(*R*)-3,3',4,4'-tetrakis(4-(*tert*-butyl)phenyl)-2*H*,2'*H*-[10,10'-bibenzo[*g*]chromene]-2,2'-dione ((*R*)-**3b**)

White solid (52 mg, 57% yield), melting point > 300 °C; ^{1}H NMR (400 MHz, $CDCl_3$) δ 8.04 (s, 1H), 7.90 (d, *J* = 8.0 Hz, 1H), 7.34-7.44 (m, 4H), 7.13-7.29 (m, 6H), 7.02-7.05 (m, 2H), 1.35 (s, 9H), 1.22 (s, 9H); ^{13}C NMR (100 MHz, $CDCl_3$) δ 161.2, 151.7, 151.4, 150.2, 148.2, 134.2, 132.0, 131.3, 130.3, 130.1, 129.7, 129.5, 129.4, 129.3, 128.4, 127.7, 125.5, 125.4, 125.2, 124.9, 124.4, 121.2, 117.2, 34.7, 34.5, 31.3, 31.2; HRMS (APCI) *m/z*: $[M+H]^+$ Calcd for $C_{66}H_{63}O_4$ 919.4721; Found 919.4751; CHIRAL ART Amylose-SA column, *n*-hexane/chloroform = 70/30, 0.2 mL/min, 25 °C, (*S*)-**3b**: t_R = 31.89 min, (*R*)-**3b**: t_R = 29.39 min, UV detection at 250.0 nm.

(*R*)-3,3',4,4'-tetrakis(4-methoxyphenyl)-2*H*,2'*H*-[10,10'-bibenzo[*g*]chromene]-2,2'-dione ((*R*)-**3c**)

White solid (57 mg, 70% yield), melting point 221-224 °C; ^{1}H NMR (400 MHz, $CDCl_3$) δ 7.97 (s, 1H), 7.86 (d, *J* = 8.0 Hz, 1H), 7.37-7.40 (m, 1H), 7.29-7.36 (m, 2H), 7.17-7.23 (m, 2H), 7.07 (dt, *J* = 8.8, 2.8 Hz, 2H), 6.90-6.99 (m, 2H), 6.73 (dt, *J* = 8.8, 2.8 Hz, 2H), 3.84 (s, 3H), 3.72 (s, 3H); ^{13}C NMR (100 MHz, $CDCl_3$) δ 161.4, 159.5, 158.8, 150.9, 148.1, 134.2, 131.9, 131.3, 131.0, 130.1, 129.4, 129.3, 128.5, 127.1, 126.6, 125.5, 125.46, 121.4, 117.1, 114.1, 113.9, 113.3, 55.3, 55.1; HRMS (APCI) *m/z* $[M+H]^+$ Calcd for $C_{50}H_{27}Br_4O_4$ 1006.8637; Found 1010.8631; CHIRAL ART Amylose-SA column, n-hexane/chloroform = 70/30, 0.5 mL/min, 25 °C, (*S*)-**3a**: t_R = 11.46 min, (*R*)-**3b**: t_R = 9.75 min, UV detection at 250.0 nm.

(*R*)-3,3',4,4'-tetrakis(4-bromophenyl)-2*H*,2'*H*-[10,10'-bibenzo[*g*]chromene]-2,2'-dione ((*R*)-**3d**)

Pale yellow solid (45 mg, 45% yield), melting point = 172-174 °C; ^{1}H NMR (400 MHz, $CDCl_3$) δ 7.85-7.90 (m, 2H), 7.54-7.63 (m, 2H), 7.31-7.48 (m, 4H), 7.12-7.27 (m, 3H), 7.01 (d, *J* = 8.4 Hz, 1H); ^{13}C NMR (100 MHz, $CDCl_3$) δ 160.5, 150.6, 147.9, 134.4, 133.3, 132.7, 132.2, 132.0, 131.33, 131.27, 131.1, 130.2, 129.6, 129.4, 129.1, 126.8, 126.0, 125.4, 123.2, 122.4, 120.4, 117.2; HRMS (APCI) *m/z*: $[M+H]^+$ Calcd for $C_{50}H_{27}Br_4O_4$ 1006.8637; Found 1010.8631; CHIRAL ART Amylose-SA column, *n*-hexane/chloroform = 70/30, 0.5 mL/min, 25 °C, (*S*)-**3d**: t_R = 11.46 min, (*R*)-**3d**: t_R = 9.75 min, UV detection at 250.0 nm.

(*R*)-3,3',4,4'-tetrakis(4-(trifluoromethyl)phenyl)-2*H*,2'*H*-[10,10'-bibenzo[*g*]chromene]-2,2'-dione ((*R*)-**3e**)

Pale yellow solid (24 mg, 25% yield), melting point = 215-219 °C; ^{1}H NMR (400 MHz, $CDCl_3$) δ 7.92 (d, J = 8.1 Hz, 1H), 7.83 (s, 1H), 7.70-7.79 (m, 2H), 7.38-7.56 (m, 6H), 7.21-7.31 (m, 3H); ^{13}C NMR (100 MHz, $CDCl_3$) δ 160.2, 150.8, 147.9, 137.9, 137.2, 134.5, 131.3, 131.0, 130.9, 130.3, 130.2, 130.1, 130.0, 129.9, 129.7, 129.5, 129.3, 126.9, 126.1, 126.0, 125.97, 125.8, 125.7, 125.4, 125.2, 125.1, 125.0, 123.7 (q, $J_{C\text{-}F}$ = 30 Hz), 123.8 (q, $J_{C\text{-}F}$ = 30 Hz), 118.0, 117.3, 117.3; ^{19}F NMR (376 MHz, $CDCl_3$) δ -62.7, -62.8, HRMS (APCI) *m/z*: $[M+H]^+$ Calcd for $C_{54}H_{27}F_{12}O_4$ 967.1712; Found 967.1734; CHIRAL ART Amylose-SA column, *n*-hexane/chloroform = 70/30, 0.2 mL/min, 25 °C, (*S*)-**3e**: t_R = 46.38 min, (*R*)-**3e**: t_R = 43.74 min, UV detection at 250.0 nm.

(*R*)-3,3',4,4'-tetra(naphthalen-2-yl)-2*H*,2'*H*-[10,10'-bibenzo[*g*]chromene]-2,2'-dione ((*R*)-**3f**)

White solid (47 mg, 52% yield), melting point > 300 °C; ^{1}H NMR (400 MHz, $CDCl_3$) δ 8.04 (bs, 1H), 7.82-7.98 (m, 4H), 7.53-7.75 (m, 4H), 7.35-7.52 (m, 5H); ^{13}C NMR (100 MHz, $CDCl_3$) δ 161.2, 151.8, 148.3, 134.4, 133.0, 132.9, 132.8, 132.6, 132.4, 132.2, 131.6, 130.4, 130.3, 129.9, 129.43, 129.38, 129.0, 128.8, 128.6, 128.5, 128.4, 128.3, 128.1, 128.02, 128.0, 127.90, 127.86, 127.6, 127.4, 127.3, 127.1, 127.0, 126.8, 126.7, 126.3, 125.9, 125.7, 125.5, 121.4, 117.3; HRMS (APCI) *m/z*: $[M+H]^+$ Calcd for $C_{66}H_{39}O_4$ 895.2843; Found 895.2854. CHIRAL ART Amylose-SA column, n-hexane/chloroform = 70/30, 0.2 mL/min, 25 °C, (*S*)-**3f**: t_R = 27.22 min, (*R*)-**3f**: t_R = 23.77 min, UV detection at 250.0 nm.

(1) For selected reviews, see: (a) Satoh, T.; Miura, M. *Chem. Eur. J.* **2010**, *16*, 11212–11222. (b) Colby, D. A.; Bergman, R. G.; Ellman, J. A. *Chem. Rev.* **2010**, *110*, 624–655. (c) Kuhl, N.; Schröder, N.; Glorius, F. *Adv. Synth. Catal.* **2014**, *356*, 1443–1460. (d) Boyarskiy, V. P.; Ryabukhin, D. S.; Bokach, N. A.; Vasilyev, A. V. *Chem. Rev.* **2016**, *116*, 5894–5986. (e) Gulías, M.; Mascareñas, J. L.; *Angew. Chem. Int. Ed.* **2016**, *55*, 11000–11019. (f) Yang, Y.; Li, K.; Cheng, Y.; Wan, D.; Li, M.; You, J. *Chem. Commun.* **2016**, *52*, 2872–2884. (g) Yoshino, T.; Matsunaga, S. *Adv. Synth. Catal.* **2017**, *359*, 1245–1262. (h) Sambiagio, C.; Schönbauer, D.; Blieck, R.; Dao-Huy, T.; Pototschnig, G.; Schaaf, P.; Wiesinger, T.; Zia, M. F.; Wencel-Delord, J.; Besset, T.; Maes, B. U. W.; Schnürch, M. *Chem. Soc. Rev.* **2018**, *47*, 6603–6743. (i) Vásquez-Céspedes, S.; Wang, X.; Glorius, F. *ACS Catal.* **2018**, *8*, 242–257. (j) Santhoshkumar, R.; Cheng, C.-H. *Chem. Eur. J.* **2019**, *25*, 9366–9384. (k) Kuang, G.; Liu, G.; Zhang, X.; Lu, N.; Peng, Y.; Xiao, Q.; Zhou, Y. *Synthesis* **2020**, *52*, 993–1006. (l) Y. Nishii, M. Miura *ACS Catal.* **2020**, *10*, 9747–9757. (m) Kumar, S.; Nunewar, S.; Oluguttula, S.; Nanduri, S.; Kanchupalli, V. *Org. Biomol. Chem.* **2021**, *19*, 1438–1458. (n) Dhawa, U.; Kaplaneris, N.; Ackermann, L. *Org. Chem. Front.* **2021**, *8*, 4886–4913.

(2) (a) Ueura, K.; Satoh, T.; Miura, M. *Org. Lett.* **2007**, *9*, 1407–1409. (b) Ueura, K.; Satoh, T.; Miura, M. *J. Org. Chem.* **2007**, *72*, 5362–5367.

(3) Li, L.; Brennessel, W. W.; Jones, W. D. *J. Am. Chem. Soc.* **2008**, *130*, 12414–12419.

(4) (a) Stuart, D. R.; Bertrand-Laperle, M.; Burgess, K. M. N.; Fagnou, K. *J. Am. Chem. Soc.* **2008**, *130*, 16474–16475. (b) Guimond, N. Fagnou, K. *J. Am. Chem. Soc.* **2009**, *131*, 12050–12051. (c) Stuart, D. R.; Alsabeh, P.; Kuhn, M.; Fagnou, K. *J. Am. Chem. Soc.* **2010**, *132*, 18326–18339.

(5) (a) Zhang, X.; Yin, J.; Yoon, J. *Chem. Rev.* **2014**, *114*, 4918–4959. (b) Tanaka, H.; Inoue, Y.; Mori, T. *ChemPhotoChem* **2018**, *2*, 386–402. (c) Dhbaibi, K.; Favereau, L.; Crassous, J. *Chem. Rev.* **2019**, *119*, 8846–8953. (d) Albano, G.; Pescitelli, G.; Bari, L. D. *Chem. Rev.* **2020**, *120*, 10145–10243. (e) Hassan, Z.; Spuling, E.; Knoll, D. M.; Lahann, J.; Bräse, S. *Chem. Soc. Rev.* **2018**, *47*, 6947–6963.

(6) (a) Takishima, R.; Nishii, Y.; Hinoue, T.; Imai, Y.; Miura, M. *Beilstein J. Org. Chem.* **2020**, *16*, 325–336. (b) Takishima, R.; Nishii, Y.; Miura, M. *Org. Lett.* **2021**, *23*, 1349–1354.

(7) For reviews, see: (a) Wagner, B. D. *Molecules* **2009**, *14*, 210–237. (b) Jung, Y.; Jung, J.; Huh, Y.; Kim, D. *J. Anal. Methods Chem.* **2018**, *2018*, 5249765. (c) Sun, X.-y.; Liu, T.; Sun, J.; Wang, X.-j. *RSC Adv.* **2020**, *10*, 10826–10847.

(8) (a) Yang, C.-W.; Hsia, T.-H.; Chen, C.-C.; Lai, C.-K.; Liu. R.-S. *Org. Lett.* **2008**, *10*, 4069–4072. (b) Chen, S.; Liu, W.; Ge, Z.; Zhang, W.; Wang, K.-P.; Hu, Z.-Q. *CrystEngComm*, **2018**, *20*, 5432–5441. (c) Shi, L.; Li, K. Cui, P.-C.; Li, L.-L.; Pan, S.-L; Li, M.-Y.; Yu. X.-Q. *J. Mater. Chem. B*, **2018**, *6*, 4413–4416. (d) Chen, S.; Liu, W.; Zhang, W.; Ge, Z.; Wang, K.-P.; Gan, L.-H.; Hu. Z.-Q. *Tetrahedron* **2019**, *75*, 3504–3509.

(9) (a) Zhao, Y.; Han, F.; Yang, L.; Xia, C. *Org. Lett.* **2015**, *17*, 1477–1480. (b) Yokoyama, Y.; Unoh, Y.; Bohmann, R. A.; Satoh, T.; Hirano, K.; Bolm, C.; Miura, M. *Chem. Lett.* **2015**, *44*, 1104–1106.

(10) For reviews, see: (a) Rajesh, P.; Sharma, K.; Katiyar, D. *Synthesis* **2016**, *48*, 2303–2322. (b) Szwaczko, K. *Inorganics* **2022**, *10*, 23.

(11) Meca, L.; Řeha, D.; Havlas, Z. *J. Org. Chem.* **2003,** *68,* 5677–5680.

(12) Li, N.; Feng, H.; Gong, Q.; Wu, C.; Zhou, H.; Huang, Z.; Yang, J.; Chen, X.; Zhao, N. *Mater. Chem. C* **2015**, *3*, 11458–11463.